Hydrogen diffusion in $GaAs_{1-x}N_x$

R. Trotta,[1] D. Giubertoni,[2] A. Polimeni,[1,*] M. Bersani,[2] M. Capizzi,[1] F. Martelli,[3] S. Rubini,[3] G. Bisognin,[4,5] and M. Berti[4]
[1]*CNISM and Dipartimento di Fisica, Sapienza Università di Roma, P.le A. Moro 2, 00185 Roma, Italy*
[2]*CMM–Fondazione Bruno Kessler–irst, via Sommarive 18, 38100 Povo Trento, Italy*
[3]*TASC-INFM-CNR, Area Science Park, S.S. 14 Km. 163.5, 34012 Trieste, Italy*
[4]*MATIS CNR-INFM and Department of Physics, University of Padova, via Marzolo 8, 35131 Padova, Italy*
[5]*CNISM, University of Padova, Padova Unit, Via Marzolo 8, 35131 Padova, Italy*
(Received 29 June 2009; revised manuscript received 14 September 2009; published 16 November 2009)

Hydrogen (or deuterium) incorporation in dilute nitride semiconductors modifies dramatically the electronic and structural properties of the crystal through the creation of nitrogen-hydrogen complexes. In this work, we investigate how the formation and dissociation of such complexes rule the diffusion of deuterium in $GaAs_{1-x}N_x$. The concentration depth profile of deuterium is determined by secondary ion mass spectrometry under a wide range of experimental conditions that comprise different N concentrations (x=0.09%, 0.40%, 0.70%, and 1.5%) and D irradiation temperatures (T_D=200, 250, 300 and 350 °C). The experimental data are successfully reproduced by a diffusion model in the presence of strong D trapping. In particular, the deuterium diffusion and capture rate coefficients are determined, and a minimum decay length of the deuterium forefront is found at low T_D (<250 °C) and high x (>0.7%). These parameters set the experimental conditions within which a nanostructuring of the physical properties of $GaAs_{1-x}N_x$ is attainable.

DOI: 10.1103/PhysRevB.80.195206 PACS number(s): 78.55.Cr, 68.49.Sf, 66.30.−h

I. INTRODUCTION

Hydrogen is an unavoidable presence in most growth and processing steps of semiconductors.[1,2] Therefore, many studies have been dedicated to the effects induced by hydrogen on the electronic and structural properties of those materials in which H can be inadvertently or purposely incorporated. Despite of its simple electronic structure, H in semiconductors exhibits an exceptionally large number of effects. For instance, it can be beneficial to the crystal optoelectronic performances by saturating dangling bonds caused by point and extended defects.[3] It has been also found that H can passivate the electrical activity of donor and acceptor impurities[1,2,4–6] and that it can act as an amphoteric impurity by itself forming acceptor and donor levels in n type and p type semiconductors, respectively.[1,7] Instead, H leads exclusively to electron conduction in InN (Refs. 8 and 9) and in most metal oxides (e.g., ZnO, CdO, La_2O_3, and $PbTiO_3$).[10,11] In these latter, an universal hydrogen pinning level was reported[10] first and extended later on to various semiconductors and insulators.[7] Another interesting debated issue concerns the surprising formation of multicenter bonds in ZnO and MgO.[12–14] Very recently, it has been shown also that bonding of hydrogen to carbon can be used to control the electrical properties of graphene.[15] Such a capability of hydrogen to tailor the properties of a material was first implemented for the fabrication of GaAs- and InP-based optical waveguides[16] and has probably the most spectacular evidence in dilute nitrides (such as, GaAsN, InGaAsN, and GaPN).[17–20]

In GaAsN,[21,22] the incorporation of a few percent of N leads to a giant reduction in the band gap energy of GaAs,[23–25] a deformation of the conduction band[26] and a puzzling compositional dependence of the parameters governing transport (i.e., electron effective mass)[27–31] and spin-related (i.e., electron effective g factor)[32,33] properties. These phenomena originate from the interaction of GaAs extended states with localized electronic levels related to single and multiple N complexes (e. g., pairs, triplets, and clusters).[34–37] Postgrowth hydrogenation of GaAsN (and GaPN) completely reverses the effects produced by N substitution of group V atoms[17–20,30,32,38] and even turns the strain of as-grown GaAsN and GaPN from tensile to compressive.[39–43] Infrared absorption measurements demonstrated that the electronic passivation of N atoms is due to the formation of N-2H complexes with C_{1h} symmetry,[44,45] where the bonds between a N atom and two Ga atoms are substituted by non equivalent bonds with two H atoms.[46,47] Nuclear reaction analyses and channeling measurements combined with high-resolution x-ray diffraction indicated that a third H atom is weakly trapped nearby an N-2H complex and is responsible for the compressive strain observed in the hydrogenated GaAsN layer.[41] Passivation of oxygen isoelectronic impurities by hydrogen was also found in ZnTeO.[48]

More recently, it has been reported that a spatial control of H incorporation (and of H-related effects) in GaAsN can be obtained by electron beam lithography-assisted deposition of metallic patterns opaque to H and successive H irradiation.[43,49–51] On the one hand, this approach opens up interesting perspectives for a nanostructuring of the electronic properties of dilute nitrides. On the other hand, it requires a deep understanding of the influence that sample properties and hydrogenation conditions play on the depth and shape of the H distribution inside the lattice. A previous work[50] based on secondary ion mass spectrometry (SIMS) and photoluminescence (PL) in $GaAs_{0.991}N_{0.009}$ showed that deuterium irradiation (in this context H and D are equivalent, but for the higher experimental sensitivity of SIMS to deuterium) is strongly influenced by the temperature, T_D, at which the sample is held during treatment. Indeed, the decay length, l_D, of the deuterium forefront sizably reduces with decreasing T_D, being as small as l_D=5 nm/decade for T_D =200 °C. Nevertheless, a systematic study of D diffusion in $GaAs_{1-x}N_x$ lacks. In particular, the diffusion parameters of D are not known and the influence of N concentration on D kinetics in the crystal has never been addressed.

In this work, we investigate deuterium diffusion at fixed deuteration temperature (T_D=300 °C) in $GaAs_{1-x}N_x$ over a wide compositional range (x=0.09%, 0.40%, 0.70%, and 1.5%) and in $GaAs_{0.993}N_{0.007}$ at varying T_D's (200, 250, 300, and 350 °C). The depth profile of the deuterium concentration is measured by SIMS. The experimental data are well-reproduced by a diffusion model that takes into account the temperature-driven interplay between formation and dissociation of various nitrogen-deuterium complexes. We find that the deuterium diffusion coefficient and capture radius are composition-independent indicating the absence of major structural modifications with increasing N concentration. Instead, these parameters vary sizably with irradiation temperature. Furthermore, the D forefront gets steeper with increasing N concentration and/or decreasing deuteration temperature. From these data, it is possible to draw a complete picture that establishes the optimal experimental conditions necessary to attain a strict control over deuterium/hydrogen diffusion in GaAsN and, hence, a spatial control at a nanometer scale of the GaAsN physical properties. Finally, we also show that photoluminescence can be properly employed to estimate the amount of GaAsN layer thickness actually passivated by hydrogen.

The paper is organized as follows. Next section reports details concerning the experimental techniques used and the sample characteristics. Section III describes the theoretical model employed to reproduce the depth profile of D concentration. Section IV focuses on the experimental data and their critical analysis. A summary of the work can be found in Sec. V.

II. EXPERIMENT

The investigated $GaAs_{1-x}N_x$ samples were grown at 500 °C by solid source molecular beam epitaxy on top of a 500-nm-thick GaAs buffer layer grown at 600 °C on a (001) GaAs substrate. The nitrogen concentrations (thicknesses) are x=0.09% (2000 nm), 0.40% (180 nm), 0.70% (180 nm), and 1.5% (180 nm). The N concentration was determined by combining PL and x-ray diffraction measurements. No GaAs cap layer was grown. All samples were D-irradiated at T_D =300 °C by a Kaufman source (100 eV ion-beam energy). Four pieces of the sample with x=0.70% were deuterated at T_D=200, 250, 300, and 350 °C, respectively (see Table I). All GaAsN layers have been only partially deuterated in order to keep the D forefront inside the N-containing layer and, thus, to allow a comparison with theoretical modeling. All deuterium irradiations were performed by using the same ion current density (25 $\mu A/cm^2$) and varying the exposure time, only—see Table I. Sample cooling rate after D irradiation was on the order of 2–3 K/s. After every irradiation, the samples were characterized by PL excited by a vanadate:Nd laser (λ=532 nm), spectrally analyzed by a 0.75-m-long monochromator and detected by a cooled InGaAs linear array detector. For SIMS measurements, a E_{Cs}=1 keV Cs^+ primary beam at oblique incidence (55°) was used in a CAMECA Sc-Ultra mass spectrometer where $^2H^-$ and $^{75}As^-$ negative secondary ions were collected with a depth resolution of 2–3 nm/decade. Other impact energies and incidence angles vs. surface normal were tested in order to individuate the best analytical conditions for this class of samples. 1 keV at 55° were the best conditions for signal to noise ratio and for depth resolution. Sputtering time was converted to an in-depth scale by measuring the obtained crater depths by a mechanical stylus profilometer. This allowed us to have an appropriate sputtering rate for the GaAsN layer that is ~10% higher with respect to the one of a pure reference GaAs layer (grown under the same conditions as GaAsN but in absence of N flux) and seemingly independent of nitrogen concentration (at least for $x \leq 1.5\%$). Secondary ion intensities of $^2H^-$ were converted to concentrations using a relative sensitivity factor (RSF) determined from the analysis of a fully deuterated sample (GaAsN epilayer with x =1.4%), whose D dose was previously measured by nuclear reaction analysis (NRA). Given the dilute N concentration, a single RSF was used independent of nitrogen content. Finally, the $^{75}As^{14}N^-$ signal, which is proportional to N concentration, varies in very good agreement with the nominal nitrogen concentration.

TABLE I. Concentration, thickness, deuterium irradiation temperature (T_D) and dose (d_D) and exposure time to D ion current (t_D) of the investigated samples.

N concentration (%)	Thickness (nm)	T_D (°C)	d_D (10^{17} cm^{-2})	t_D (s)
0.09	2000	300	3.0	2090
0.4	180	300	0.60	440
0.4	180	300	2.0	1440
0.7	180	200	2.4	1700
0.7	180	250	1.7	1170
0.7	180	300	1.2	870
0.7	180	350	0.20	150
1.5	180	300	2.5	1800

III. THEORETICAL MODEL

On the ground of previous studies,[41] we know that the interaction of D with N leads to the formation of (N-2D)-D complexes where: (i) two D atoms bind to a single N atom forming a very stable N-2D complex, which is responsible for the electronic passivation of nitrogen and (ii) a third D atom is more weakly trapped nearby passivated N atoms and causes a compressive strain in the GaAsN layer (the exact position of this satellite D atom is unknown, yet). Careful x-ray diffraction measurements on deuterated GaAsN samples subjected to different thermal annealings showed that the third D atom is removed from its site at 250 °C with an activation energy equal to 1.77 eV.[42] At the same time, the compressive strain disappears while N atoms are still electronically passivated (namely, the band gap energy of GaAsN:D is equal to that of GaAs). A higher activation energy (=1.89 eV) (Ref. 42) characterizes, instead, the dissociation of the N-2D complexes and the concomitant recovery of the GaAsN pristine properties, e.g., band gap energy value.[41]

Diffusion of deuterium in a solid can be modeled by the one dimensional Fick's equation given by

$$\frac{\partial n_{\mathrm{D}}}{\partial t} = D_{\mathrm{dif}} \frac{\partial^2 n_{\mathrm{D}}}{\partial z^2}, \tag{1}$$

where z indicates the depth coordinate, n_{D} is the deuterium concentration, and D_{dif} is the diffusion coefficient of deuterium in that material. In the case of a semi-infinite medium, extending from $z=0$ (sample surface) to $z \to \infty$, with a constant concentration of deuterium at $z=0$, n_{D0}, the solution to Eq. (1) is the complementary error function $n_{\mathrm{D}}=n_{\mathrm{D0}}\,\mathrm{erfc}(Y)$ with $Y=z\sqrt{1/(4D_{\mathrm{dif}}\,t)}$. However, this solution does not account for D diffusion in GaAsN. Indeed, D kinetics in GaAsN is ruled by a multiple trapping process,[2,50,52] where capture ceases as soon as three D atoms bind to one N atom in accordance with preceding experimental results.[41,42] This multiple trapping of D by N results in a concentration plateau, which is not reproduced by Eq. (1), as shown by the dotted line in Fig. 1. Therefore, one has to take into account trapping as well as kind and thermal stability of the D-related complexes formed. We treat the GaAsN epilayer as a semi-infinite medium occupying the $z \geq 0$ space. Let n_{D} be the concentration of free (i.e., unbound) D atoms, $n_{\mathrm{N}i\mathrm{D}}$ be the concentration of N atoms with $i=1,2,3$ D atoms bonded and n_{N} be the concentration of D-free N atoms such that N_{N}

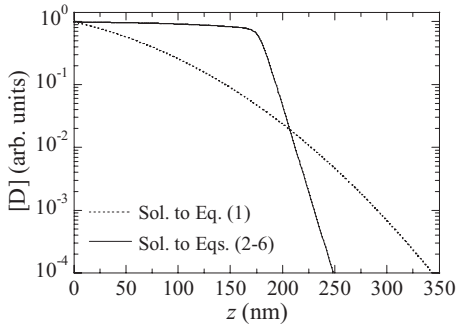

FIG. 1. Calculated deuterium concentration as a function of depth (sample surface $z=0$) in a GaAsN layer with N concentration $x=0.7\%$. The dotted line is the solution for a purely diffusive motion given by Eq. (1). The solid line corresponds to D diffusion in the presence of the multiple-trapping processes described by Eqs. (2)–(6). A same diffusion coefficient $D_{\mathrm{dif}}=2.6\times10^{-12}$ cm^2 s^{-1} but different diffusion times were employed: $t=15$ s for free diffusion and $t=3500$ s for diffusion in the presence of trapping. Notice the absence of a plateau in the purely diffusive case and the steep forefront when multiple D trapping is included.

$=[\Sigma_{i=1,3} n_{\mathrm{N}i\mathrm{D}}(z,t)+n_{\mathrm{N}}(z,t)]$, where N_{N} is the spatially uniform concentration of nitrogen. For $x \geq 0$ and $t \geq 0$, the time (and space for unbound D, only) evolution of the involved species is given by

$$\frac{\partial n_{\mathrm{D}}}{\partial t} - D_{\mathrm{dif}} \frac{\partial^2 n_{\mathrm{D}}}{\partial z^2} = -k\left(n_{\mathrm{D}} n_{\mathrm{N}} + n_{\mathrm{D}} n_{\mathrm{ND}} + n_{\mathrm{D}} n_{\mathrm{N2D}}\right) + \gamma_a n_{\mathrm{N3D}} + \gamma_b n_{\mathrm{N2D}} + \gamma_c n_{\mathrm{ND}} \quad \bullet \; n_{\mathrm{D}} \tag{2}$$

$$\frac{\partial n_{\mathrm{N}}}{\partial t} = -k n_{\mathrm{D}} n_{\mathrm{N}} + \gamma_c n_{\mathrm{ND}} \quad \bigcirc \; n_{\mathrm{N}} \tag{3}$$

$$\frac{\partial n_{\mathrm{ND}}}{\partial t} = k n_{\mathrm{D}} n_{\mathrm{N}} - \gamma_c n_{\mathrm{ND}} - k n_{\mathrm{D}} n_{\mathrm{ND}} + \gamma_b n_{\mathrm{N2D}} \quad \bigcirc \; n_{\mathrm{ND}} \tag{4}$$

$$\frac{\partial n_{\mathrm{N2D}}}{\partial t} = k n_{\mathrm{D}} n_{\mathrm{ND}} - k n_{\mathrm{D}} n_{\mathrm{N2D}} + \gamma_a n_{\mathrm{N3D}} - \gamma_b n_{\mathrm{N2D}} \quad \bigcirc \; n_{\mathrm{N2D}} \tag{5}$$

$$\frac{\partial n_{\mathrm{N3D}}}{\partial t} = k n_{\mathrm{D}} n_{\mathrm{N2D}} - \gamma_a n_{\mathrm{N3D}} \quad \bigcirc \; n_{\mathrm{N2D}} \tag{6}$$

On top of each term in Eqs. (2)–(6), a sketch of the corresponding complex transformations considered is depicted. Large (gray) and small (black) circles indicate N and D atoms, respectively. An arrow pointing toward N indicates the formation of an N–D bond. The breaking of an N–D bond is represented by a doubly crossed line. On the right-hand side of Eq. (2), the first term in parenthesis represents the capture of one D atom by N atoms having i (=0,1,2) D atoms already bonded. $k=4\pi r D_{\mathrm{dif}}$ is the capture rate coefficient,[52] where r is an effective capture radius and D_{dif} is the diffusion coefficient of deuterium in $GaAs_{1-x}N_x$. For simplicity purposes, we keep a same k for each trapping step. The second, third and fourth term in the order account for the thermal release of one D atom from an (N-2D)-D, an N-2D and an

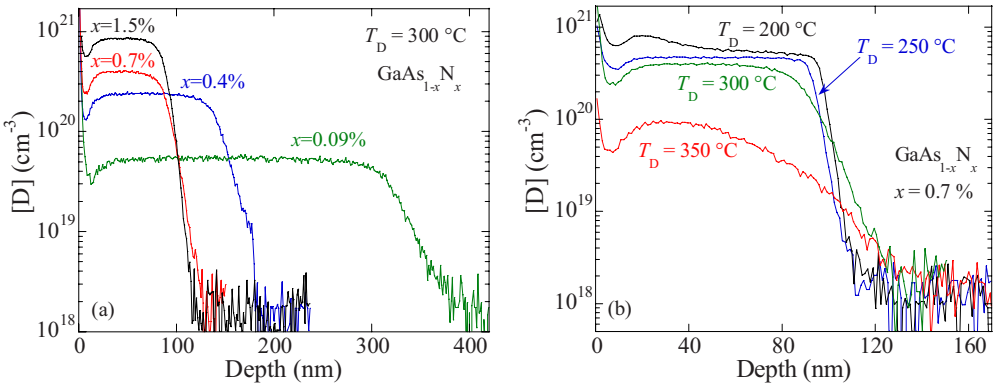

FIG. 2. (Color online) (a) SIMS depth profile of deuterium concentration (0 corresponds to sample surface) for $GaAs_{1-x}N_x$ samples with different N concentration x. The sample irradiation temperature was T_D=300 °C. (b) Same as (a) for x=0.7% and different irradiation temperatures.

N-D complex, respectively. The dissociation rate can be written as[52] $\gamma_m = \nu e^{-E_m/k_B T}$, where ν is the attempt frequency and E_m (with m=a,b,c) is the activation energy for the release of one D atom from the specific complex considered. As mentioned above, previous experiments disclosed the existence of *two* steps in the dissolution of (N-2D)-D complexes.[41,42] In the first step, one D atom is removed with activation energy E_a leaving an N-2D complex, in the second step the N-2D complex is dissociated by releasing the remaining two D atoms (thus, leaving an unpassivated N atom). Therefore, we will effectively assume $\gamma_a \neq \gamma_b = \gamma_c$. This implies that in the N-2D complex the second and third D atoms are released with a same activation energy, $E_b = E_c$. Finally, Eqs. (3)–(6) represent the time evolution of the *immobile* $n_{NiD}(z,t)$ species.

Equations (2)–(6) form a system of five coupled partial-differential equations that can be solved numerically. It should be noticed that the above equations are not independent of each other and the system can be reduced from 5 to 4 equations, simply exploiting the condition $\partial N_N / \partial t = 0$, where $N_N = [\Sigma_{i=1,3} n_{NiD}(z,t) + n_N]$. We solve the reduced system of differential equations using the following initial and boundary conditions: $n_{NiD}(z,0)=0$ (for $z>0$) and $n_N(z,0)=N_N$ for $z>0$, $n_D(0,t)$=const (set by the current of impinging D^+ ions during the experiment), $n_N(0,t)=0$, and $n_D(\infty,t) = n_{ND}(\infty,t) = n_{N2D}(\infty,t) = n_{N3D}(\infty,t) = 0$. The total deuterium depth profile is given by

$$n_D^{tot}(z) = n_D + \sum_{i=1,3} i n_{NiD}(z). \quad (7)$$

Figure 1 compares the deuterium profile obtained in a GaAsN sample by solving Eqs. (2)–(6) with that derived from Eq. (1); a same D_{dif} was used with different diffusion times. At variance with the solution of the simple Fick's equation, the present model leads to a deuterium plateau followed by an exponential-like decay, as previously reported in the case of a trap limited diffusion with negligible complex dissociation.[53] *We emphasize, finally, that* D_{dif} determines mainly the depth position of the knee preceding the exponential decay of the D concentration, while r influences primarily the slope l_D of the D forefront.[53]

IV. RESULTS AND DISCUSSION

The main experimental data considered in this work are shown in Fig. 2. Firstly, notice that the D concentration peak at the surface is an artificial feature of SIMS. Furthermore, the concentration weakening at 10–15 nm below the surface is in part (see Sec. IV B) due to the instability of the sputtering rate and ion yield during the initial stages of SIMS measurements. Panel (a) displays the deuterium profile along the $GaAs_{1-x}N_x$ growth direction in all samples after irradiation at T_D=300 °C. The D profile exhibits a concentration plateau, whose value is proportional to x, and a forefront that gets sharper as x increases. Figure 2(b) shows the evolution of the D concentration profile upon varying T_D between 200 °C and 350 °C for x=0.7%. Incorporation at lower temperatures results in steeper D profiles. In particular, at T_D =200 °C deuterium tends to accumulate near the sample surface, while a D depletion develops at higher T_D's (such depletion partly overlaps the artificial concentration weakening mentioned above).

Next, we provide the reader with some details concerning the data analysis performed and in the following subsections we will discuss the physical implications of the results presented in Fig. 2.

The quite rich picture emerging from SIMS data requires a quantitative analysis of the D concentration profiles. The resolution of the CAMECA system for E_{Cs}=1 keV can be assumed as 2.5 nm/decade. Therefore, a deconvolution of the experimental data is helpful to derive the true D concentration profile. This is particularly significant when the depth resolution approaches the decay length of the diffused species, such as in the case of samples having a high nitrogen concentration ($x>0.7\%$) and/or treated at low temperature ($T_D<300$ °C). Then, we model the measured data $n_{D,exp}^{tot}(z)$ by a convolution of a response function $R(z)$ with the true concentration profile $n_D^{tot}(z)$ derived from Eqs. (2)–(7),

$$n_{D,exp}^{tot}(z) = \int_0^\infty n_D^{tot}(z') R(z-z') dz'. \quad (8)$$

We choose the response function following the works of Dowsett and co-workers,[54,55] who showed that SIMS re-

sponses for a wide range of impurities and matrices can be modeled by

$$R(z) = \frac{1}{2\lambda}[1 + \mathrm{erfc}(\xi)]\exp[-z/\lambda + (\sigma/\lambda)^2/2], \qquad (9)$$

where erfc(ξ) is the complementary error function and $\xi = 2^{-1/2}(z/\sigma - \sigma/\lambda)$. σ and λ take into account, respectively, broadening and shift in the measured profile with respect to the true profile caused by the ion-beam induced mass-transport that occurs during sample profiling. Ideally, one should derive the values of σ and λ by measuring a deuterium δ-like layer, a procedure that unfortunately cannot be followed in our case. Therefore, we estimate these parameters by convolving an ideal steplike profile with Eq. (8) and imposing that the resulting profile has a decay length equal to 2.5 nm/decade, namely equal to the resolution of the CAMECA system for $E_{Cs}=1$ keV. By this approach, we derive $\sigma=1.0$ nm and $\lambda=1.13$ nm. These values compare reasonably well with those reported for $E_{Cs}=2.4$ keV in GaAs.[56]

A. Dependence of deuterium depth profile on nitrogen concentration

Figure 3 shows an enlargement of the SIMS data (symbols) around the trailing edge of the deuterium profile in samples having different nitrogen concentration but the same deuteration temperature ($T_D=300$ °C); see Fig. 2(a). The dotted lines represent the true concentration profiles $n_D^{tot}(z)$ as estimated by solving the system of partial differential equations reported above, while the solid lines are the convolutions $n_{D,exp}^{tot}(z)$ of the true profiles with the system response, as given by Eqs. (8) and (9). We obtain a very good agreement between model and experiments. In the simulation procedure we fixed the diffusion time equal to the duration of the sample exposure to deuterium ions, the N concentration equal to the nominal value of the GaAsN samples and $\nu = 90$ THz (Ref. 39) for the detrapping processes mentioned in Sec. III. E_m, r and D_{dif} are treated as free parameters. The only pair of activation energies that fit all data [comprising those shown in Fig. 2(b); see next section] is $E_a = (1.75 \pm 0.03)$ eV and $E_b = (2.0 \pm 0.1)$ eV.[57] These values are in agreement with those derived from previous structural studies.[42]

The quantitative agreement observed in Fig. 3 between the calculated and experimental deuterium concentration supports the correctness of the formation and dissociation processes included in Eqs. (2)–(6) and inferred by other experiments.[41,42,44–46] Indeed, the stoichiometric ratio, $q = [D]/[N]$, between the deuterium concentration at the plateau and the N concentration gives a sample-averaged value $q=2.7$ that varies little with x. This value supports the formation of (N-2D)-D complexes as dominant species at $T_D = 300$ °C and it is in accordance with that reported in Ref. 41, where nuclear reaction analysis was performed in similar samples.

Figures 4(a) and 4(b) show the compositional dependence of the capture radius and diffusion coefficient, respectively. In doped semiconductors, one does not expect a variation of these parameters with trap (i.e., dopant) concentration. A similar result is found here for $GaAs_{1-x}N_x$ with $x = (0.09-1.5)\%$. Somehow this is a surprising result. In fact, dilute nitrides undergo major changes in their electronic properties and, above all, a strong local deformation on the N lattice sites with increasing N concentration, even in a very narrow compositional window (0%–1%). Other alloy phenomena, such as phase separation and strain relaxation may occur as well. These latter could affect heavily the kinetics of deuterium, in particular the diffusion coefficient and capture rate. The independence of these parameters on N concentration indicate that lattice relaxation following N incorporation does not influence them and that other "disruptive" structural changes do not occur up to a N concentration equal to 1.5%.

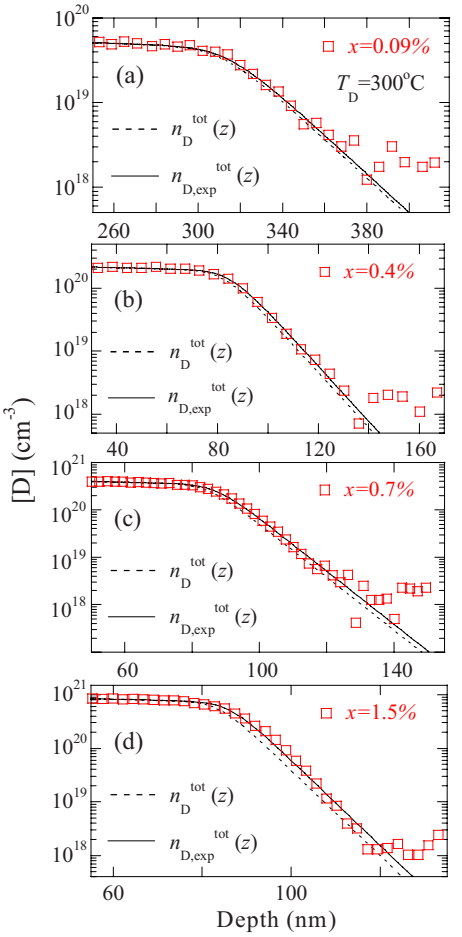

FIG. 3. (Color online) Enlargement of the SIMS depth profile (squares) at the forefront of the D trailing edge in $GaAs_{1-x}N_x$ samples with x equal to (a) 0.09%, (b) 0.4%, (c) 0.7%, and (d) 1.5%. D irradiation temperature $T_D=300$ °C in all cases. The dashed lines are a simulation to the data by Eqs. (2)–(7). The solid lines are convolutions of the calculated profile with the SIMS response function according to Eqs. (8) and (9). Notice the different depth scales with varying x.

Interestingly, Fig. 3 shows that the slope l_D of the D forefront decreases sizably with increasing N concentration. This indicates that, being D_{dif} and r basically independent of x, the concentration of traps is mainly responsible for the knee depth and lineshape of the deuterium concentration profile in the lattice. We will come back on l_D when we will analyze the dependence of SIMS on deuteration temperature.

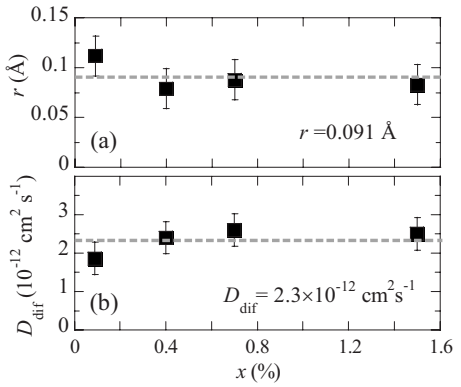

FIG. 4. Dependence on nitrogen concentration of the (a) N capture radius r of deuterium and (b) deuterium diffusion coefficient D_{dif}. These values have been derived by the simulations shown in Fig. 3. The horizontal dashed lines indicate the mean value of these quantities (also reported in the figure).

B. Dependence of deuterium depth profile on deuterium irradiation temperature

The dependence of the D concentration profile on irradiation temperature is shown in Fig. 5 for the 180-nm-thick $GaAs_{0.007}N_{0.993}$ sample. Different impinging doses at fixed ion current density were employed in order to let deuterium travel a similar distance in the lattice, independently of T_{D} (see Table I). Different phenomena occur during D diffusion, such as the temperature-driven formation and breaking of (N-2D)-D and N-2D complexes and the ensuing capture/release of D atoms by/from these complexes. The solid lines are a convolution of the true D concentration profiles $n_{\mathrm{D}}^{\mathrm{tot}}(z)$ with the SIMS response; see Eqs. (8) and (9). The not-convoluted solution of the diffusion model given by solving Eqs. (2)–(7) is shown by dotted lines. The values of the activation energies E_m (1.75 eV for m=a and 2.0 eV for m=b and c) are the same as those derived by the compositional dependence of the D concentration profiles (see Fig. 3). The diffusion coefficient and capture radius of deuterium have been used as adjustable parameters.

The simulation misses the D accumulation observed close to the sample surface at the lowest T_{D} and its progressive depletion at higher T_{D}'s (see Fig. 2). Deuterium accumulation could be due to interstitial D atoms or molecules (not considered by our model), which form when the incoming flux of D atoms in not completely balanced by D diffusion inside the sample. Deuterium surface depletion is most likely due, instead, to D out-diffusion from the sample. The importance of this process increases with T_{D} thus affecting more and more the D concentration in the first (10–15) nm from the surface. Apart from these features, the calculations reproduce extremely well the experimental results, but for T_{D} =350 °C. At this temperature, the lineshape of the D deuterium distribution changes qualitatively since the dissociation process involving N-2D complexes enters into play sizably.[42] Our model reproduces only approximately the lineshape for T_{D}=350 °C. According to simulations, this mismatch cannot be reproduced by either the sample "annealing" that occurs during the cool down time following the turn-off of the D ion current or by deuterium out-diffusion. The worse agreement

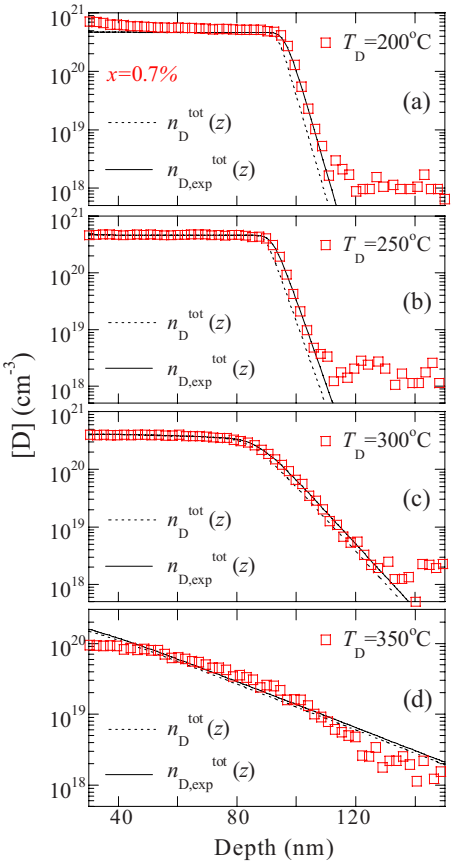

FIG. 5. (Color online) Enlargement of the SIMS depth profile (squares) at the forefront of the D trailing edge in a $GaAs_{1-x}N_x$ sample with x=0.7% and undergone to different D irradiation temperatures: (a) 200 °C, (b) 250 °C, (c) 300 °C, and (d) 350 °C. The dashed lines are simulations to the data by Eqs. (2)–(7). The solid lines are convolutions of the calculated profile with the SIMS response function according to Eqs. (8) and (9).

between simulation and SIMS data at 350 °C could be tentatively justified by supposing that some of the assumptions we made in our model (e.g., same capture radius for each trapping step or same activation energy for the release of the second and third D atom in the N-2D complex) are no longer fully valid at high temperature. We feel that these assumptions (and their partial failure at high temperature) may be related to the approaching of the trapping-detrapping regime.[53]

Figures 6(a) and 6(b) show, respectively, the dependence of r and D_{diff} on deuteration temperature. A decrease of r with increasing T_{D} is observed. This is likely due to a lowered capability of N atoms to capture D atoms, determined by thermal agitation. Eventually this leads to a broader D forefront (namely, greater l_{D}). D_{dif} decreases with T_{D} as found in previous studies,[1,2,52,58,59] although a quantitative comparison is made difficult because of the quite different results obtained by different authors.

The data presented so far concern the total deuterium concentration, $n_{\mathrm{D}}^{\mathrm{tot}}(z)$, since this is the only quantity that can be directly monitored by SIMS. Nevertheless, the solution of Eqs. (2)–(6) provides the concentration of all the species involved in the diffusion process. Now, we focus our atten-

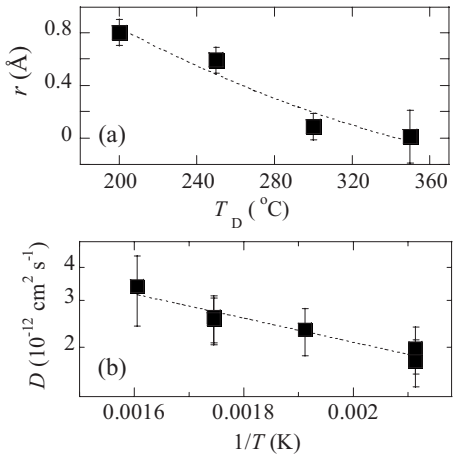

FIG. 6. Dependence on deuterium irradiation temperature of (a) N capture radius r of deuterium and (b) deuterium diffusion coefficient D_{dif}. These values have been derived by the simulations shown in Fig. 5. The dashed lines are guides to the eye.

tion on their evolution with temperature, highlighting the importance of the detrapping terms present in the diffusion equations. Figure 7 shows the concentration of the various species (n_D, n_N, n_{ND}, n_{N2D}, and n_{N3D}) present in Eqs. (2)–(6). According to Eq. (7) the weighted sum of these contributions gives the total concentration of D atoms. The curves displayed in Fig. 7 have been extracted from the simulations of the D concentration profiles measured for $x=0.7\%$ at different T_D's (see Fig. 5). Some interesting aspects can be outlined. (i) There is almost no unbound deuterium (n_D) inside the sample at all deuteration temperatures. This is consistent with the absence of other traps different from N, as also verified by SIMS measurements in a deuterated N-free GaAs reference (not shown here), where no D could be detected. (ii) The concentration of D-free nitrogen (n_N) is close to zero up to the trailing edge of the D depth profile for $T_D=(200-300)$ °C. At the highest temperature, the increased dissociation of N-iD complexes leads to a relatively greater value of n_N. (iii) The N-D complex (n_{ND}) is confined for all T_D's at the trailing edge of the D depth profile, where the trapping and detrapping processes are still completing. (iv) As regards to the N-2D (n_{N2D}) and (N-2D)-D (n_{N3D}) complexes a continuous evolution with the irradiation temperature can be noted. Starting from $T_D=200$ °C we observe that (N-2D)-D dominates in the D-containing region of the sample, while N-2D is forming at the D forefront. By increasing the temperature (250 °C÷300 °C), the (N-2D)-D complexes start to dissociate (corresponding to the first detrapping process with activation energy equal to $E_a=1.75$ eV) and the relative importance of the N-2D species increases. Furthermore, all the species profiles are broader and the resulting trailing edge of the total deuterium concentration is less steep. As the temperature is increased further, the (N-2D)-D complexes dissolve almost completely and the second de-trapping process comes into play (activation energy equal to $E_b=E_c=2.0$ eV) dissociating the N-2D complex, too. As a result, a small concentration of free nitrogen (and unbound deuterium) atoms are found nearby the surface of the sample.

These findings parallel nicely the PL and X-ray diffraction data summarized in the first paragraph of Sec. III.

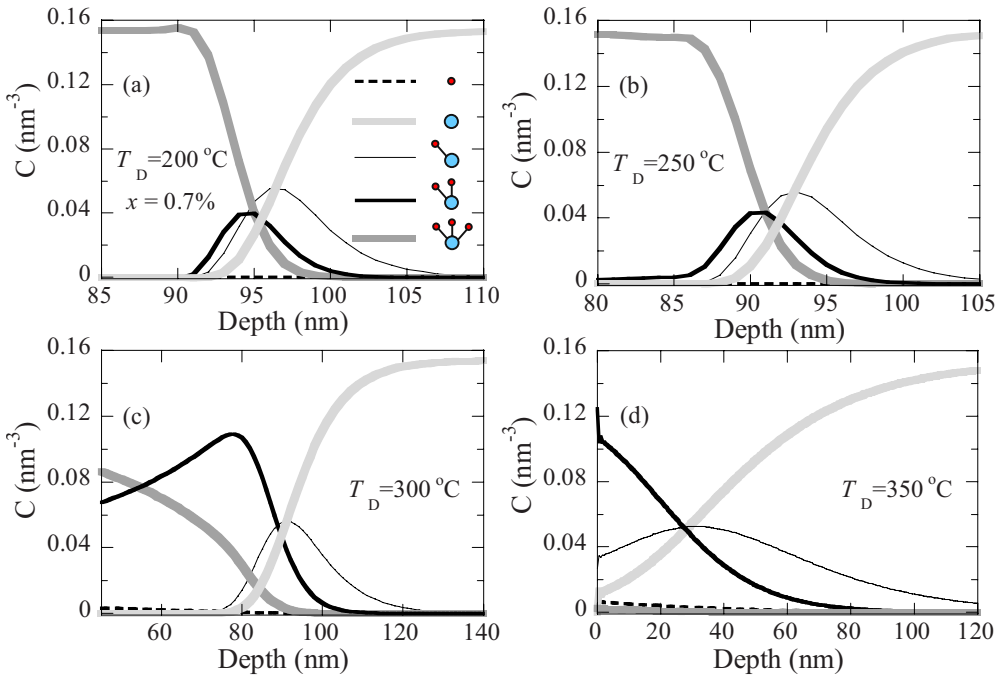

FIG. 7. (Color online) Depth dependence of the concentration of the various species (n_D, n_N, n_{ND}, n_{N2D}, and n_{N3D}) involved in the diffusion of deuterium. The different lines have been extracted from the simulations of the D concentration profiles measured for $x=0.7\%$ at different T_D's (see Fig. 5): (a) 200 °C, (b) 250 °C, (c) 300 °C, and (d) 350 °C. The inset of panel (a) depicts the correspondence.

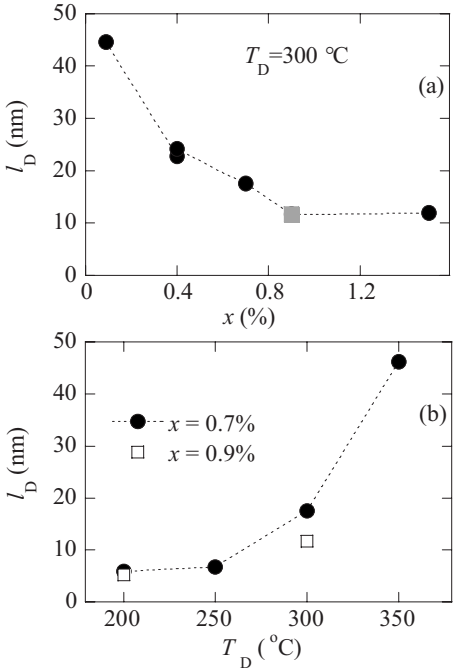

FIG. 8. (a) Compositional dependence of the D decay length l_D, defined as the length within which the D concentration decreases by a factor 10 in the exponential-like region starting from half of its maximum concentration. The gray square refers to the 0.9% sample reported in Ref. 50. (b) Irradiation temperature dependence of l_D in the x=0.7% (full circles) and x=0.9% samples (open squares refers to the 0.9% sample reported in Ref. 50).

C. Deuterium decay length and optical properties of deuterated $GaAs_{1-x}N_x$

The results reported so far show that a control of the electronic and structural properties of dilute nitrides can be obtained at a nanometer scale provided that a sufficiently low deuteration temperature and high N concentration are used. Therefore, site-, shape- and size-controlled nanostructures or strain engineering[43] could be obtained by suitable deposition of H-opaque metallic masks prior to H exposure.[49–51] By using a similar approach, adjacent planar regions having different refractive index values[38] could be realized in order to achieve photon waveguiding.[16] For these applications, a most significant parameter is given by the decay length of the D forefront into the sample. In fact, the sharpness of the deuterium profile determines ultimately the confinement profile of carriers and photons. Figures 8(a) and 8(b) show the dependence of D decay length l_D (defined as the length within which the D concentration decreases by a factor 10 in its exponential-like decay on starting from half of its maximum concentration) on nitrogen concentration and deuteration temperature, respectively. By varying the nitrogen concentration at fixed temperature (300 °C), the decay length decreases progressively from 45 nm/decade (x=0.09%) to 10 nm/decade for $x>0.7\%$ consistently with the higher density of traps. For x=0.7%, l_D increases from 5.8 nm/decade to 18 nm/decade when the sample deuteration temperature is augmented from 200 to 300 °C. In particular, a more abrupt increase in the decay length is observed when going from

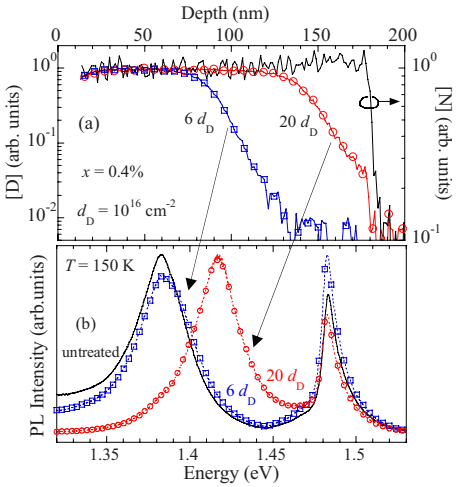

FIG. 9. (Color online) (a) SIMS depth profiles of deuterium (left axis) and nitrogen (right axis) in the x=0.4% sample. The sample irradiation temperature was 300 °C and two different ion impinging doses were employed: lower dose (squares, $d_D=6\times10^{16}$ cm^{-2}) and higher dose (circles, $d_D=2\times10^{17}$ cm^{-2}). (b) Photoluminescence, PL, spectrum at 150 K of the untreated sample (solid line), of the low-dose deuterated sample (dashed line and squares, $d_D=6\times10^{16}$ cm^{-2}), and of the high-dose deuterated sample (dashed line and circles, $d_D=2\times10^{17}$ cm^{-2}). The SIMS data of the latter two samples are shown in panel (a). The PL bands peaked at about 1.38 eV correspond to carrier recombining in deuterium-free GaAsN. The PL peak at about 1.48 eV is due to carrier recombination in GaAs or fully passivated GaAsN regions. The band at about 1.42 eV originates from carrier recombining in the sample region located at the deuterium forefront, where a partial passivation of N atoms occurred.

T_D=300 °C to T_D=350 °C.[60] This is caused by the fact that in this temperature interval basically all (N-2D)-D complexes are dissociated and a sizable number of N-2D complexes start being broken [see Fig. 7(d)]. Then, the diminished capability of N atoms to retain D atoms at high temperature (corresponding to smaller r and greater D_{dif} values) gives rise to a much broad D forefront.

The steepness and shape of the D trailing edge reflects on the sample optical properties, too. In particular, in synergy with SIMS, PL can be usefully used to estimate the extent of the D-free GaAsN thickness after irradiation. Figure 9(a) shows the SIMS depth profiles of deuterium and nitrogen for x=0.4%. The sample irradiation temperature was 300 °C and two different ion impinging doses were employed by using the same ion current but different exposure times. This results in a nearly rigid shift in the D concentration trailing edge in the sample treated with the greater D dose. Then, the deuterium concentration drops to the noise level at the GaAsN/GaAs interface. The PL spectra at 150 K of the two samples are shown in Fig. 9(b) along with that of the untreated GaAsN. The peak energy of the GaAsN-related emission is the same in the untreated and in the low-dose irradiated sample. However, the weight of the GaAs-related emission is slightly higher in the latter sample due to the reduced thickness of the GaAsN layer. We point out that in a PL experiment carriers relax toward regions of the sample having the lowest band gap energy before recombining ra-

diatively. As reported in Ref. 49, the carrier diffusion length in $GaAs_{1-x}N_x$ (x=0.5%) ranges between 0.6 μm (at 4.2 K) and 1.8 μm (at room temperature), namely, much more than the thickness (0.18 μm) of the x=0.4% sample, whose PL spectra are shown in Fig. 9(a). In the sample deuterated at lower dose (open squares in Fig. 9), no sizable carrier recombination occurs in the fully or partially deuterated regions closer to the sample surface and almost all luminescence originates from the D-free 50-nm-thick GaAsN layer at the GaAsN/GaAs interface. In the sample irradiated at higher D dose, the low-energy band due to GaAsN is blue-shifted by about 40 meV, as if a smaller N concentration were achieved. SIMS data disclose the origin of this blue-shift as due to a partial N passivation occurring at the interface between the GaAsN and GaAs buffer layers (the fully passivated GaAsN layer closer to the sample surface has a band gap energy resonant with that of the GaAs buffer). Consequently, a fine tuning of the effective N concentration in dilute nitrides can be realized especially in GaAsN epilayers with small N concentration[29,61] or in GaAsN (or InGaAsN) quantum wells.[17,18] In the latter heterostructures, one exploits the small thickness of the well (usually a few nm) in order to vary quite uniformly the density of electronically active N atoms.

V. CONCLUSIONS

We have presented a comprehensive study of deuterium (hydrogen) diffusion in $GaAs_{1-x}N_x$ by secondary ion mass spectrometry for a trap concentration regime (2×10^{22} cm^{-3}) going beyond that possible in impurity-doped semiconductors. We have found that both N concentration (x=0.09%–1.5%) and irradiation temperature (T_D =200–350 °C) play a major role in determining the distance covered by D and the lineshape of the D forefront in the lattice. Deuterium concentration profiles have been simulated by a diffusion model in the presence of strong trapping. The experimental data are successfully reproduced provided that the correct stoichiometry and thermal stability of the formed nitrogen-deuterium complexes are taken into account. We have found a deuterium diffusion coefficient and an effective capture radius, respectively, equal to $D_{dif}=(2.3\pm0.4)\times10^{-12}$ cm^2 s^{-1} and $r=(0.09\pm0.03)$ Å at T_D=300 °C. These parameters do not depend sizably on N concentration. Instead, D_{dif} and r increases and decreases, respectively, with deuteration temperature. A very steep (5 nm/decade) D forefront is observed at low irradiation temperature (200 °C) and high N concentration ($x>0.7\%$). These results allow us to predict the extent as well as shape of deuterium (or hydrogen) forefront in dilute nitrides. This is of uttermost importance in the engineering of dilute nitride-based nanostructures and optical waveguides that could be realized by means of spatially selective hydrogenation.

ACKNOWLEDGMENTS

This work was supported by the Transnational Access program of the EU project "European Integrated Activity of Excellence and Networking for Nano and Micro-Electronics Analysis" ANNA under Contract No. 026134 (RII3).

*antonio.polimeni@romal.infn.it

[1] *Hydrogen in Semiconductors, Semiconductors and Semimetals*, edited by J. I. Pankove and N. M. Johnson (Academic Press, Boston, 1991), Vol. 34.
[2] J. Pearton, J. W. Corbett, and M. Stavola, *Hydrogen in Crystalline Semiconductors* (Springer-Verlag, Berlin, 1992).
[3] A. Polimeni, D. Marangio, M. Capizzi, A. Frova, and F. Martelli, Appl. Phys. Lett. **65**, 1254 (1994).
[4] J. Chevallier, W. C. Dautremont-Smith, C. W. Tu, and S. J. Pearton, Appl. Phys. Lett. **47**, 108 (1985).
[5] J. I. Pankove, D. E. Carlson, J. E. Berkeyheiser, and R. O. Wance, Phys. Rev. Lett. **51**, 2224 (1983).
[6] A. Y. Polyakov, N. B. Smirnov, A. V. Govorkov, K. H. Baik, S. J. Pearton, B. Luo, F. Ren, and J. M. Zavada, J. Appl. Phys. **94**, 3960 (2003).
[7] C. G. Van de Walle and J. Neugebauer, Nature (London) **423**, 626 (2003).
[8] A. Janotti and C. G. Van de Walle, Appl. Phys. Lett. **92**, 032104 (2008).
[9] G. Pettinari, F. Masia, M. Capizzi, A. Polimeni, M. Losurdo, G. Bruno, T. H. Kim, S. Choi, A. Brown, V. Lebedev, V. Cimalla, and O. Ambacher, Phys. Rev. B **77**, 125207 (2008).
[10] Ç. Kılıç and A. Zunger, Appl. Phys. Lett. **81**, 73 (2002).
[11] K. Xiong, J. Robertson, and S. J. Clark, J. Appl. Phys. **102**, 083710 (2007).
[12] Anderson Janotti and Chris G. Van de Walle, Nature Mater. **6**, 44 (2007).
[13] H. Takenaka and D. J. Singh, Phys. Rev. B **75**, 241102(R) (2007).
[14] M.-H. Du and D. J. Singh, Phys. Rev. B **79**, 205201 (2009).
[15] D. C. Elias, R. R. Nair, T. M. G. Mohiuddin, S. V. Morozov, P. Blake, M. P. Halsall, A. C. Ferrari, D. W. Boukhvalov, M. I. Katsnelson, A. K. Geim, and K. S. Novoselov, Science **323**, 610 (2009).
[16] M. Kumar, J. T. Boyd, H. E. Jackson, J. M. Zavada, H. A. Jenkinson, R. G. Wilson, B. Theys, and J. Chevallier, J. Appl. Phys. **82**, 3205 (1997).
[17] A. Polimeni, G. Baldassarri H. v., H. M. Bissiri, M. Capizzi, M. Fischer, M. Reinhardt, and A. Forchel, Phys. Rev. B **63**, 201304(R) (2001).
[18] G. Baldassarri H. v. H., M. Bissiri, A. Polimeni, M. Capizzi, M. Fischer, M. Reinhardt, and A. Forchel, Appl. Phys. Lett. **78**, 3472 (2001).
[19] M. Bissiri, G. B. von Högersthal, A. Polimeni, M. Capizzi, D. Gollub, M. Fischer, M. Reinhardt, and A. Forchel, Phys. Rev. B **66**, 033311 (2002).
[20] A. Polimeni, M. Bissiri, M. Felici, M. Capizzi, I. A. Buyanova, W. M. Chen, H. P. Xin, and C. W. Tu, Phys. Rev. B **67**, 201303(R) (2003).
[21] *Physics and Applications of Dilute Nitrides*, edited by I. A. Buy-

anova and W. M. Chen (Taylor & Francis, New York, 2004).
[22] *Dilute Nitride Semiconductors*, edited by M. Henini (Elsevier, Oxford, UK, 2005).
[23] W. Shan, W. Walukiewicz, J. W. Ager, E. E. Haller, J. F. Geisz, D. J. Friedman, J. M. Olson, and Sarah R. Kurtz, Phys. Rev. Lett. **82**, 1221 (1999).
[24] U. Tisch, E. Finkman, and J. Salzman, Appl. Phys. Lett. **81**, 463 (2002).
[25] T. Taliercio, R. Intartaglia, B. Gil, P. Lefebvre, T. Bretagnon, U. Tisch, E. Finkman, J. Salzman, M.-A. Pinault, M. Laügt, and E. Tourniè, Phys. Rev. B **69**, 073303 (2004).
[26] J. Endicott, A. Patanè, J. Ibáñez, L. Eaves, M. Bissiri, M. Hopkinson, R. Airey, and G. Hill, Phys. Rev. Lett. **91**, 126802 (2003).
[27] G. B. von Högersthal, A. Polimeni, F. Masia, M. Bissiri, M. Capizzi, D. Gollub, M. Fischer, and A. Forchel, Phys. Rev. B **67**, 233304(R) (2003).
[28] F. Masia, A. Polimeni, G. Baldassarri Höger von Högersthal, M. Bissiri, M. Capizzi, P. J. Klar, and W. Stolz, Appl. Phys. Lett. **82**, 4474 (2003).
[29] A. Polimeni, A. Baldassarri Hoeger von Hoegersthal, F. Masia, A. Frova, M. Capizzi, S. Sanna, V. Fiorentini, P. J. Klar, and W. Stolz, Phys. Rev. B **69**, 041201(R) (2004).
[30] F. Masia, G. Pettinari, A. Polimeni, M. Felici, A. Miriametro, M. Capizzi, A. Lindsay, S. B. Healy, E. P. O'Reilly, A. Cristofoli, G. Bais, M. Piccin, S. Rubini, F. Martelli, A. Franciosi, P. J. Klar, K. Volz, and W. Stolz, Phys. Rev. B **73**, 073201 (2006).
[31] A. Patanè, G. Allison, N. V. Kozlova, Q. D. Zhuang, A. Krier, M. Hopkinson, and G. Hill, Appl. Phys. Lett. **93**, 252106 (2008).
[32] G. Pettinari, F. Masia, A. Polimeni, M. Felici, A. Frova, M. Capizzi, A. Lindsay, E. P. O'Reilly, P. J. Klar, W. Stolz, G. Bais, M. Piccin, S. Rubini, F. Martelli, and A. Franciosi, Phys. Rev. B **74**, 245202 (2006).
[33] H. M. Zhao, L. Lombez, B. L. Liu, B. Q. Sun, Q. K. Xue, D. M. Chen, and X. Marie, Appl. Phys. Lett. **95**, 041911 (2009).
[34] P. R. C. Kent and A. Zunger, Phys. Rev. Lett. **86**, 2613 (2001); Phys. Rev. B **64**, 115208 (2001).
[35] G. Pettinari, A. Polimeni, F. Masia, R. Trotta, M. Felici, M. Capizzi, T. Niebling, W. Stolz, and P. J. Klar, Phys. Rev. Lett. **98**, 146402 (2007).
[36] A. Lindsay and E. P. O'Reilly, Phys. Rev. Lett. **93**, 196402 (2004).
[37] E. P. O' Reilly, A. Lindsay, P. J. Klar, A. Polimeni, and M. Capizzi, Semicond. Sci. Technol. **24**, 033001 (2009).
[38] M. Geddo, T. Ciabattoni, G. Guizzetti, M. Galli, M. Patrini, A. Polimeni, R. Trotta, M. Capizzi, G. Bais, M. Piccin, S. Rubini, F. Martelli, and A. Franciosi, Appl. Phys. Lett. **90**, 091907 (2007).
[39] P. J. Klar, H. Grüning, M. Güngerich, W. Heimbrodt, J. Koch, T. Torunski, W. Stolz, A. Polimeni, and M. Capizzi, Phys. Rev. B **67**, 121206(R) (2003).
[40] G. Bisognin, D. De Salvador, A. V. Drigo, E. Napoletani, A. Sambo, M. Berti, A. Polimeni, M. Felici, M. Capizzi, M. Güngerich, P. J. Klar, G. Bais, F. Jabeen, M. Piccin, S. Rubini, F. Martelli, and A. Franciosi, Appl. Phys. Lett. **89**, 061904 (2006).
[41] M. Berti, G. Bisognin, D. DeSalvador, E. Napolitani, S. Vangelista, A. Polimeni, M. Capizzi, F. Boscherini, G. Ciatto, S. Rubini, F. Martelli, and A. Franciosi, Phys. Rev. B **76**, 205323 (2007).
[42] G. Bisognin, D. De Salvador, E. Napolitani, M. Berti, A. Polimeni, M. Capizzi, S. Rubini, F. Martelli, and A. Franciosi, J. Appl. Crystallogr. **41**, 366 (2008).
[43] R. Trotta, A. Polimeni, M. Capizzi, F. Martelli, S. Rubini, M. Francardi, A. Gerardino, and L. Mariucci, Appl. Phys. Lett. **94**, 261905 (2009).
[44] F. Jiang, M. Stavola, M. Capizzi, A. Polimeni, A. Amore Bonapasta, and F. Filippone, Phys. Rev. B **69**, 041309(R) (2004).
[45] S. Kleekajai, F. Jiang, K. Colon, M. Stavola, W. B. Fowler, K. R. Martin, A. Polimeni, M. Capizzi, Y. G. Hong, H. P. Xin, C. W. Tu, G. Bais, S. Rubini, and F. Martelli, Phys. Rev. B **77**, 085213 (2008).
[46] G. Ciatto, F. Boscherini, A. A. Bonapasta, F. Filippone, A. Polimeni, and M. Capizzi, Phys. Rev. B **71**, 201301(R) (2005).
[47] A. Amore Bonapasta, F. Filippone, and G. Mattioli, Phys. Rev. Lett. **98**, 206403 (2007).
[48] M. Felici, A. Polimeni, M. Capizzi, Y. Nabetani, T. Okuno, K. Aoki, T. Kato, T. Matsumoto, and T. Hirai, Appl. Phys. Lett. **88**, 101910 (2006).
[49] M. Felici, A. Polimeni, G. Salviati, L. Lazzarini, N. Armani, F. Masia, M. Capizzi, F. Martelli, M. Lazzarino, G. Bais, M. Piccin, S. Rubini, and A. Franciosi, Adv. Mater. **18**, 1993 (2006).
[50] R. Trotta, A. Polimeni, M. Capizzi, D. Giubertoni, M. Bersani, G. Bisognin, M. Berti, S. Rubini, F. Martelli, L. Mariucci, M. Francardi, and A. Gerardino, Appl. Phys. Lett. **92**, 221901 (2008).
[51] L. Felisari, V. Grillo, F. Martelli, R. Trotta, A. Polimeni, M. Capizzi, F. Jabeen, and L. Mariucci, Appl. Phys. Lett. **93**, 102116 (2008).
[52] R. A. Morrow, J. Appl. Phys. **66**, 2973 (1989).
[53] M. S. Janson, A. Hallén, M. K. Linnarsson, and B. G. Svensson, Phys. Rev. B **64**, 195202 (2001).
[54] M. G. Dowsett and D. P. Chu, J. Vac. Sci. Technol. B **16**, 377 (1998).
[55] M. G. Dowsett and R. Collins, Philos. Trans. R. Soc. London, Ser. A **354**, 2713 (1996).
[56] M. G. Dowsett, G. Rowlands, P. N. Allen, and R. D. Barlow, Surf. Interface Anal. **21**, 310 (1994).
[57] The larger uncertainty on E_b is due to the lower sensitivity of SIMS simulations on this parameter for $T_D \leq 300$ °C. Indeed, the dissociation process of N-2D complexes is fully activated at higher temperature.
[58] J. M. Zavada, H. A. Jenkinson, R. G. Sarkis, and R. G. Wilson, J. Appl. Phys. **58**, 3731 (1985).
[59] J. Räisänen, J. Keinonen, V. Karttunen, and I. Koponen, J. Appl. Phys. **64**, 2334 (1988).
[60] Although an exponential decay is not observed for $T_D = 350$ °C, l_D is the length within which the D concentration decreases by a factor 10 on starting from half of its maximum concentration.
[61] A. Polimeni, F. Masia, G. Pettinari, R. Trotta, M. Felici, M. Capizzi, A. Lindsay, E. P. O'Reilly, T. Niebling, W. Stolz, and P. J. Klar, Phys. Rev. B **77**, 155213 (2008).